Molecular Crystals and Liquid Crystals Science and Technology. Section A. Molecular Crystals and Liquid Crystals

Publication details, including instructions for authors and subscription information:
http://www.tandfonline.com/loi/gmcl19

Statistical Characterization of Laser Generated Instabilities in a Nematic Liquid Crystal Film

Carlo Versace [a], Vincenzo Carbone [a], Gabriella Cipparrone [a], Cesare Umeton [a] & Roberto Bartolino [a]

[a] Dipartimento di Fisica, Università della Calabria e Istituto Nazionale di Fisica della Materia Unità di Cosenza, 87036, Rende, CS, Italy

Version of record first published: 24 Sep 2006.

To cite this article: Carlo Versace , Vincenzo Carbone , Gabriella Cipparrone , Cesare Umeton & Roberto Bartolino (1996): Statistical Characterization of Laser Generated Instabilities in a Nematic Liquid Crystal Film, Molecular Crystals and Liquid Crystals Science and Technology. Section A. Molecular Crystals and Liquid Crystals, 290:1, 267-299

To link to this article: http://dx.doi.org/10.1080/10587259608031912

Mol. Cryst. Liq. Cryst., 1996, Vol. 290, pp. 267–299
Reprints available directly from the publisher
Photocopying permitted by license only

STATISTICAL CHARACTERIZATION OF LASER GENERATED INSTABILITIES IN A NEMATIC LIQUID CRYSTAL FILM.

CARLO VERSACE, VINCENZO CARBONE, GABRIELLA CIPPARRONE, CESARE UMETON AND ROBERTO BARTOLINO
Dipartimento di Fisica, Università della Calabria e Istituto Nazionale di Fisica della Materia Unità di Cosenza, 87036 Rende CS, Italy

Abstract In this paper we investigate the chaotic dynamics occurring in a nematic liquid crystal film during the director reorientation induced by an intense optical field. The experimental evidence of intermittency in the phenomenon of the molecular director reorientation is reported. It is demonstrated that the fluctuations of the transmitted light intensity I(t) follow a non-normal distribution and, by calculating the q-th power of the structure functions of I(t), the multifractal structure of the attractor is characterized. On the basis of these results, a heuristic model for the energy exchange between the radiation and the matter is introduced, which is based on a two-scale Cantor set with equal partition intervals.

INTRODUCTION

Nematic Liquid Crystals (NLC) are ordered fluids whose mean local molecular orientation can be expressed, on a length scale of the same order of the visible light wavelength , by a vectorial field $\vec{n}(\vec{r})$ called the director. Their response to an external perturbation gives rise to several collective phenomena that often result in a distortion of the local mean molecular orientation $\vec{n}(\vec{r})$. It is well known that the molecular director reorientation can be induced by external static electric and magnetic fields[1,2] as well as by an optical field[3]. In particular, the interaction with an intense optical field can exhibit different features depending on the experimental geometry, e.g., the unperturbed directors orientation (homeotropic, planar or hybrid), the polarization of the incident light and the incidence

angle. For example, if the electric field of the incident light is perpendicular to the unperturbed director, the distortion sets in only if the strength of the optical field exceeds a given well-defined threshold value; this kind of transition is called light induced Freedericksz transition[3] (LIFT). Since the birefringence of the NLC depends on the director orientation, a nonlinear phenomenon occurs: by changing the director orientation, the light beam modifies the refractive indexes of the medium, thus changing the spatial pattern of the transmitted beam (self-phase modulation effect[4]). This effect, with a particular geometry, results in several oscillating diffraction rings that can be observed in the pattern of the transmitted beam. Light, on the other hand, represents a helpful tool to investigate the dynamics of the NLC director since, in a given geometry and once the polarization of the incident beam has been fixed, a precise (even if, generally, very complicated) dependence on the director orientation exists for the intensity and the polarization of the light revealed in different points of the transmitted beam pattern[5].

At present the above mentioned oscillating behavior has been observed in two experimental geometries.

1- When a circularly or elliptically polarized light beam acts on a homeotropically aligned NLC film at normal incidence[6,7,8].

2- When a linearly polarized light beam impinges on a homeotropically aligned NLC film at a small incidence angle and the light polarization is perpendicular to the incidence plane[9,10,11].

The first experimental geometry has been exhaustively studied by Santamato and coworkers[6,7,8]. Both for elliptical and circular polarizations of the light, if the intensity of the impinging laser beam exceeds the threshold value, a time dependent variation of the transmitted beam polarization has been observed, which reflects the orientational dynamics of the director. These effects are interpreted in terms of an angular momentum exchange between the optical and the director fields, by accounting for the balance or the imbalance of optical, elastic and viscous torques in the medium. When the incident light beam has circular polarization, it causes both a distortion and a uniform precession of the molecular director about the direction of propagation of the light[6] . The case of elliptical polarization[7]

differs from that of circular polarization mainly because the molecular reorientation breaks the azimuthal symmetry of the system giving rise to several dynamic regimes, i.e., nutation and non uniform precession. For elliptical as well as circular polarization the motion of $\vec{n}(\vec{r})$ results, in the phase space, in a limit cycle sustained by the balance between the energy supplied to the NLC by the radiation and the energy dissipated as a result of the viscosity. The angular velocity of $\vec{n}(\vec{r})$ is a function of the impinging intensity, so that several limit cycles are possible, but no evidence of an instability of these limit cycles has been reported.

The existence of a limit cycle has been also reported[11] for the second experimental geometry. In this case the self oscillations are strictly periodic only in a well-defined range of the laser intensity and of the incidence angles. Outside this range, the fluctuations become stochastic. The authors investigated experimentally the regime of the periodic oscillations while nothing, except the observation of "irregular self oscillations" of the transmitted pattern, has been reported about the "stochastic regime".

For the same geometry (oblique incidence of a linearly polarized ordinary beam), in previous papers[12] we have reported the observation and a first characterization of the various dynamic regimes occurring in the system when the limit cycle becomes unstable.

The study was performed by detecting, in the center of the transmitted beam, the intensities ($I_{\perp}$ and $I_{//}$) of the two components polarized respectively perpendicular and parallel to the polarization of the incident beam. When the light intensity exceeds the threshold value, the molecular director reorients out of the incidence plane, so that the medium appears birefringent to the incident light, whose polarization becomes elliptical while passing through the sample.

The analysis of the time behavior of $I_{\perp}$ and $I_{//}$ shows several interesting features: as the light intensity is increased (over the LIFT threshold), the system at first undergoes an incomplete period doubling cascade, then a biperiodic regime appears and, finally, the transition to a chaotic regime occurs.

In this paper we are concerned with the characterization of the chaotic regime in the same experimental geometry.

Many dynamic systems exhibit a transient behavior followed by an asymptotic motion lying on an attractor in the phase space on which the orbits converge[13]. However, when the dynamic system becomes very complicated and the dimensionality of the problem increases, this kind of description is no longer feasible and a more accurate characterization is necessary. It may happen that the time evolution of the signal no longer remains quasi periodic but instead becomes chaotic[13]. At this stage a more specific characterization of the system can be given in terms of the set of Lyapunov exponents, which represent the long-term evolution of the radius of an infinitesimal sphere of states in the phase space. For a chaotic system, neighboring orbits in the phase space diverge exponentially, indicating that the system is extremely sensitive to the initial conditions. In a chaotic dynamic system, like, for example, the celebrated Lorenz system, one can extract from the signal an underlying one dimensional map. Even if this map might contain some useful information about the system, the study of the map, which is necessarily non-invertible, cannot provide a complete description of the dynamics of the system.

In the last few years a new method to describe the structure of chaotic attractors has been introduced. It consists in the determination of the multifractal structure of the attractor, if any exists[15]. Indeed, the attractor generally lies on a fractal set of non integer dimension, i.e., the measure created on the attractor is singular on the various scales of the phase space, and the singularity lies on a set of non integer dimension. Often the orbit does not fill uniformly the attractor, so that its fractal dimension (generally the so called "information dimension") cannot give an accurate description of its structure. To gain more insight one can account for a distribution of singularities of the measure created on the strange attractor, all lying on sets of different fractal dimensions. A multifractal description of this kind has indeed proved to be useful in the characterization of the structure of attractors in dynamic systems[14,15] , and in particular the knowledge of the spectrum of singularities, i.e., the spectrum of the fractal dimensions on the different scales of the attractor, has been viewed as a universal feature, similar to a class of universal maps for the chaotic dynamic systems.

The plan of this paper is the following: In section 2 we give the description of the experiment and we report the qualitative characterization of the various observed dynamic

regimes. In accordance with the previous remarks the measured time series, their power spectra and their projections on the phase space are reported. In section 3 the estimate of the maximum Lyapunov exponent and that of the information dimension is given in the chaotic regime. Our analysis shows that, as the impinging power is increased, the system behaves more like a chaotic state, so that in the following we restrict our survey to the structure of the strange attractor.

In section 4 we analyze $I_{\perp}(t)$ and $I_{//}(t)$ on different time scales and show that the signal $I_{\perp}(t)$, unlike $I_{//}(t)$, proves to be self similar and intermittent. In section 5 we summarize the theoretical approach to the analysis of the multifractal structure of an attractor; then the method is used to characterize the attractors of $I_{\perp}(t)$ and $I_{//}(t)$.

Finally, in section 6, we summarize our results and, by using a simple model, we show that, on the basis of the experiments, the phenomenon of the molecular reorientation can be modelled by a binomial multiplicative process.

DESCRIPTION OF THE EXPERIMENT

The experimental geometry is sketched in figure 1. The light beam (TEM_{00}) from an Argon ion laser (λ = 5145Å) is focused on the sample by a 150 mm focal length lens. The light beam is polarized perpendicularly to the incidence plane (ordinary wave) and its incidence angle Φ is fixed to 7°.

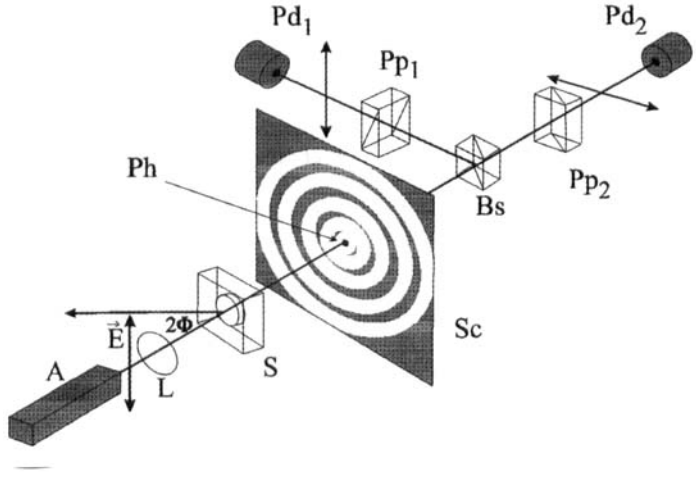

FIGURE 1: experimental setup, A = Ar+ laser, L = Lens, S = nematic liquid crystal sample and oven, Sc = Screen, Ph = pinhole, Pd_1 and Pd_2 = photodiodes, Pp_1 and Pp_2 = polarizing prisms, Bs = beamsplitter.

The sample cell consists of two optical glass flats held together by two metal clips and spaced by four Mylar spacers,50 μm thick. In order to achieve a uniform homeotropic alignment the surfaces of the optical flats have been coated by a polymeric surfactant (by Kisso Corporation). The cell has been filled by capillarity with the nematic liquid crystal material, which is an eutectic mixture of cyanobiphenyl compounds (E7 by British Drug Houses).

By means of a thermostatic bath, the temperature of the sample is held constant at the value of 18 ± 0.5 °C. We can not prevent, however, local heating of the sample, due to a very small absorption of the laser light, that might occur at the highest intensities of the incident light.

By means of a beamsplitter and two crossed polarizers we analyze $I_{\perp}(t)$ and $I_{//}(t)$, which are the components of the transmitted beam polarized perpendicularly and parallelly to the polarization of the incident beam. Since we are interested only to the light transmitted along the incidence direction, each beam is filtered by a 200 μm pinhole placed just in its center. Both $I_{\perp}(t)$ and $I_{//}(t)$ are detected by two photodiodes and sent to a personal computer that enable their AD conversion and the storage for further processing. Every time series consists of N = 16384 points that are sampled at the fixed time interval $\Delta\tau = 0.1$ seconds.

In figures 2 and 3 we report the oscillating time behavior of $I_{\perp}$ and $I_{//}$ for three different values of the power P_{inc} of the incident laser beam. The Fourier spectra and the projection of the signals on the phase space defined by $(I, dI/dt)$ are also shown. At the lowest light intensity ($P_{inc} \approx$ 420 mW) we get the signals shown in figures 2a and 3a, whose spectra

S(ω) show a single fundamental frequency indicating a sharp periodic pulsation that results in a limit cycle in the phase space. As the light intensity is increased the limit cycle become unstable and the spectra exhibit several sharp frequencies (see figures 2b and 3b that refer to $P_{inc} \approx$ 540 mW). Finally, at higher values of P_{inc} the peaks broaden and the gaps between them become shallower. The latter regime exhibits, in the phase space, a chaotic motion on a strange attractor (sees figures 2c and 3c obtained at $P_{inc} \approx$ 700 mW).

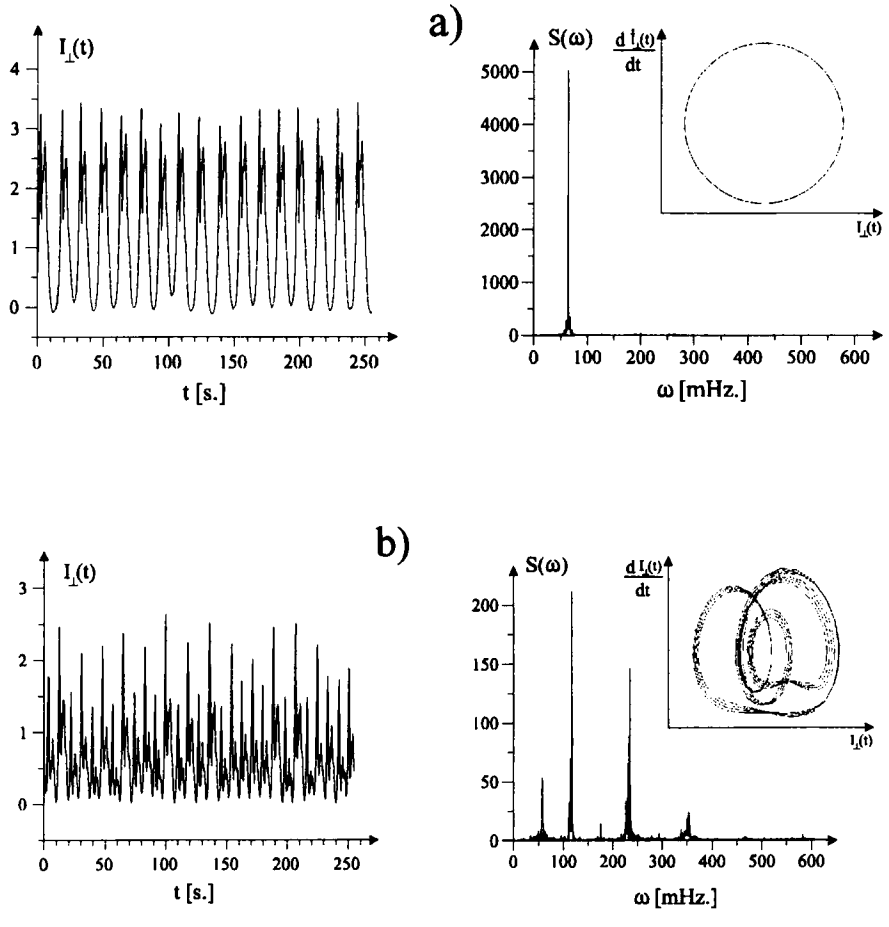

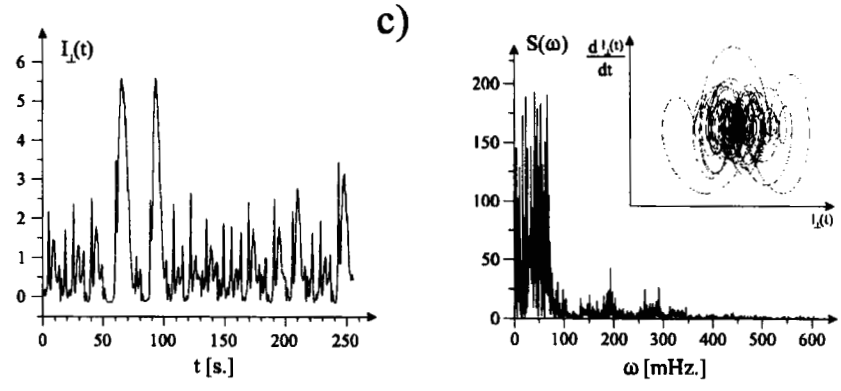

FIGURE 2: Time behavior of the signals $I_\perp$, the frequency spectrum $S(\omega)$ and the trajectory in the phase space $\left(I_\perp, dI_\perp / dt\right)$ for three different values of the impinging power: a) 420 mW, b) 540 mW, c) 700 mW.

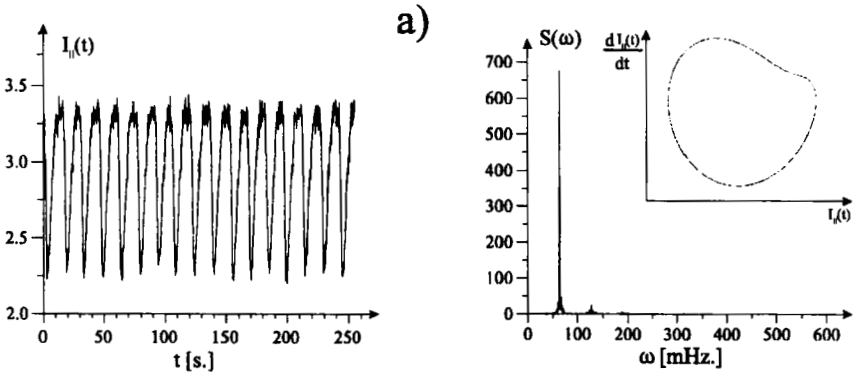

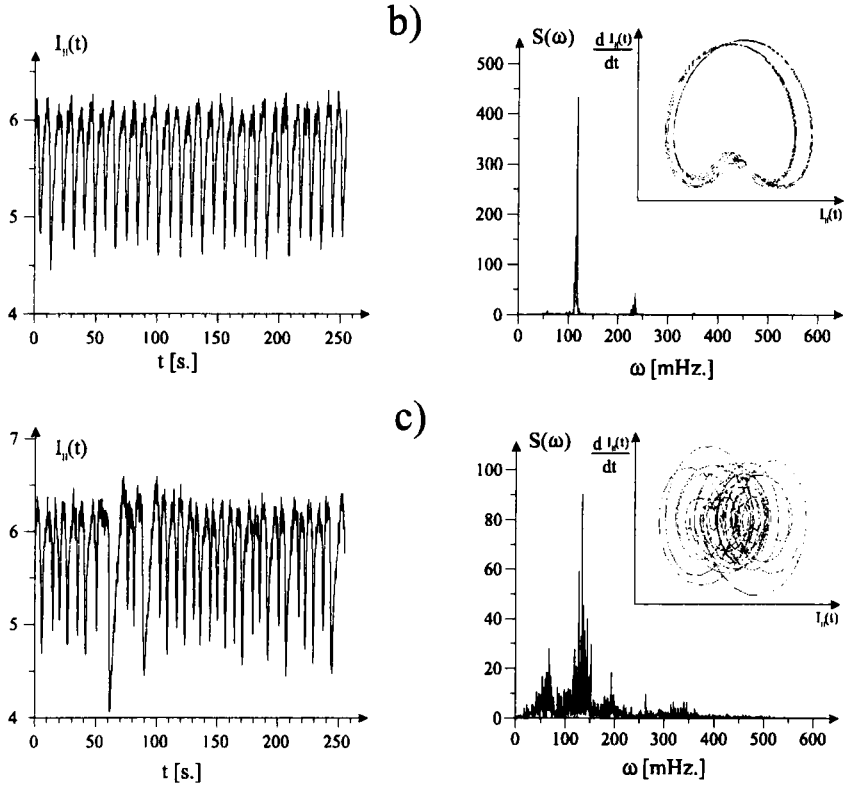

FIGURE 3: Time behavior of the signals $I_{//}$, the frequency spectrum $S(\omega)$ and the trajectory in the phase space $\left(I_{//}, dI_{//}/dt\right)$ for three different values of the impinging power: a) 420 mW, b) 540 mW, c) 700 mW.

GLOBAL ANALYSIS OF THE CHAOTIC REGIME

We are interested in the analysis of the global dynamic properties of the chaotic regime performed by the study of the structure of the low dimensional strange attractor, if any

exists. For this reason in the following we shall consider only those measures of $I_{\perp}$ and $I_{//}$, which have been performed in the chaotic regime ($P_{inc} \approx 700$ mW).

In figure 4 we show the autocorrelation coefficients $\rho_\tau(I_{//})$ and $\rho_\tau(I_{\perp})$, defined by:

$$\rho_\tau(x) = \frac{C_\tau(x)}{C_0(x)}$$

where

$$C_\tau(x) = \langle x(t+\tau)\, x(t)\rangle - \langle x(t+\tau)\rangle\langle x(t)\rangle.$$

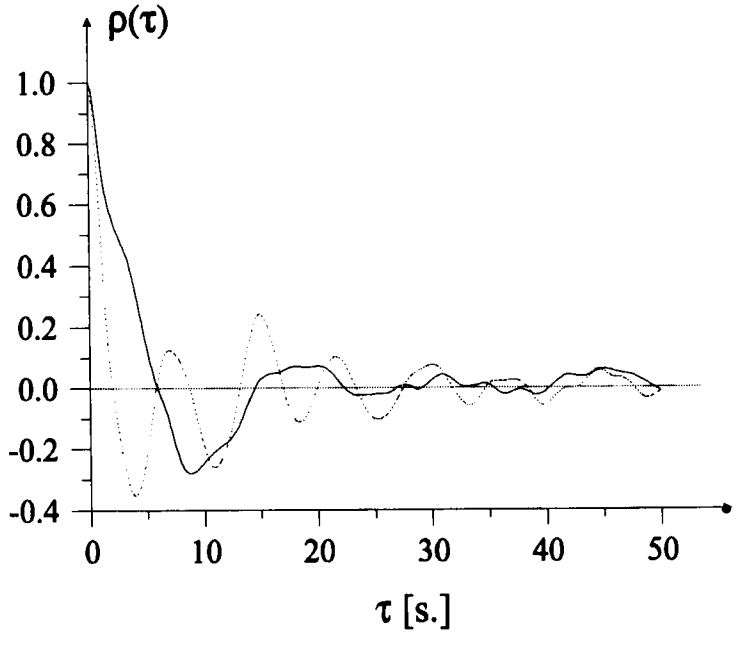

FIGURE 4: Autocorrelation coefficients $\rho(\tau)$ both of $I_{//}$ (dotted line) and $I_{\perp}$ (full line).

It is clear that both $I_{//}$ and $I_{\perp}$, drawn by the dotted and the continuous curves respectively, lose correlation in a short time, just as we expect for a deterministic random signal, being about 4s the e-folding time of $\rho_\tau(I_\perp)$ and about 2s that of $\rho_\tau(I_{//})$.

The conventional approach to the reconstruction of the dynamic properties of a measured chaotic signal, consists of two main steps[13]: the determination of the fractal dimension of the attractor and the determination of, at least, the largest Lyapunov exponent of the trajectory embedded in the phase space.

According to the embedding theorem of Takens[16], if the dynamics of a complex system can be reduced to the low dimensional one described by a differential equation of the form:

$$\frac{d\vec{x}(t)}{dt} = f(\vec{x},\gamma)$$

(where $\vec{x}(t)$ is the vector of the observable dynamic variables, f is a nonlinear function and γ is an external control parameter) its dynamics can be experimentally reconstructed from the observed time series. Therefore, following the method suggested by Takens,[16] we have reconstructed the orbit on the attractor in the embedding phase space[17,18] taking the projection of the experimental dynamic system on a d_E dimensional phase space R^{dE}. For a suitably chosen lag time τ we have formed, both for $I_{//}$ and $I_{\perp}$, the d_E-tuples

$$\vec{x}(I,t) = \{I(t), I(t+\tau), \ldots, I(t+(d_E-1)\tau)\}$$

Each vector $\vec{x}(I,t)$ represents a point in the embedding phase space of dimension d_E and the time evolution of $\vec{x}(I,t)$ maps out the orbit on the attractor in that phase space. In order to estimate the fractal dimension of the attractors given by $\vec{x}(I_\perp,t)$ and $\vec{x}(I_{//},t)$, we have used the well known method of Grassberger and Procaccia[19], i.e., by means of the $N_P = N - d_E(\tau/\Delta\tau) + 1$ points of the vector $\vec{x}(t)$, we have computed the correlation sum

$$C(r) = \frac{1}{N_P^2}\left\{\begin{array}{l}\text{the number of pairs } \vec{x}(t_i) \text{ and } \vec{x}(t_j) \text{ such that}\\ \text{the distance among the pair is less than } r\end{array}\right\} = \frac{1}{N_P^2}\sum_{i,j}\Theta\left(r - \left\|\vec{x}_i - \vec{x}_j\right\|\right)$$

where Θ is the Heaviside function. As Grassberger and Procaccia showed, the information dimension ν of the attractor can be found from the relation $C(r) \approx r^{\nu(1)}$. If the embedding dimension d_E is large enough, the slope of the plot of $\mathrm{Log}[C(r)]$ vs $\mathrm{Log}(r)$ settles down to a value that does not depend on d_E (Takens[16] showed that it suffices $d_E > 2\nu+1$). Then we calculated the value of n by a least-squares fit in the linear range of the log-log plot.

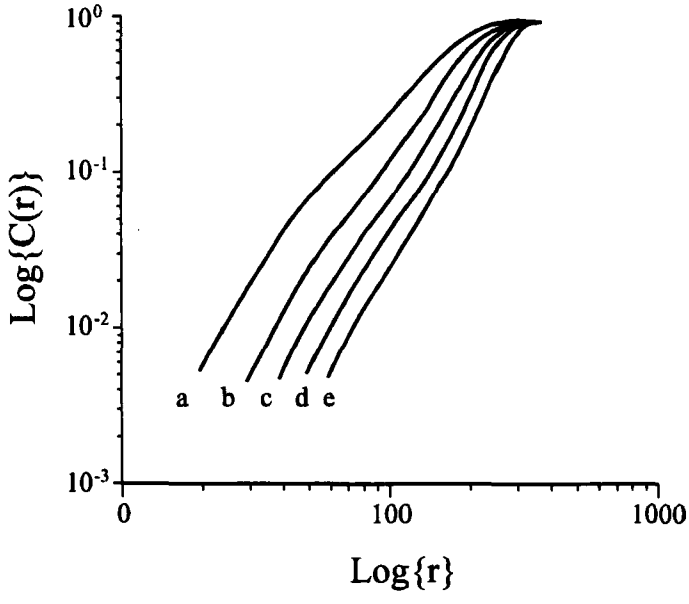

FIGURE 5a : The logarithmic plot of the correlation sum $C(r)$ vs. r for $I_{//}$ is shown for five values of the embedding dimension: d_E: a) d_E =5, b) d_E =7, c) d_E =9, d) d_E =11, e) d_E = 13.

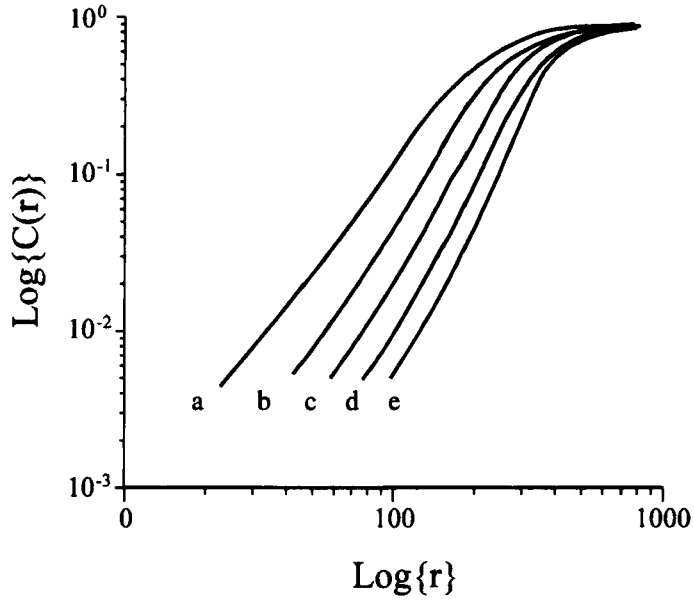

FIGURE 5b: The logarithmic plot of the correlation sum C(r) vs. r for $I_\perp$ is shown for five different values of the embedding dimension: d_E: a) d_E =5, b) d_E =7, c) d_E =9, d) d_E =11, e) d_E = 13.

In figures 5a and 5b the curves Log[C(r)] vs Log(r) are plotted for different values of d_E both for $I_{//}$ and $I_\perp$. When $d_E \geq 8$ the slopes $\nu(I_\perp)$ and $\nu(I_{//})$ of the linear part of the curves in figures 5a and 5b converge to the fractal values $\nu(I_\perp) = 3.4 \pm 0.1$ and $\nu(I_{//}) = 3.1 \pm 0.1$. This fact is evident from figure 6 where $\nu(I_\perp)$ and $\nu(I_{//})$ are reported as a function of the embedding dimension d_E. For the lag time in our calculations we have chosen the e-folding time of the signal autocorrelation functions, that is 4 seconds for $I_\perp$ and 2 seconds for $I_{//}$.

We have repeated the same calculations by using, as lag times, t=8.8 seconds and t=6.2 seconds, which correspond to the first minimum of the autocorrelation functions $\rho_\tau(I_\perp)$ and $\rho_\tau(I_{//})$ respectively, and we get the same values of ν. It is worth remarking that, because the estimate of the fractal dimension ν depends on the number N of points that constitute the time series, often it could be altered by the small number of available experimental points. A reasonable minimum number N_{min} has been estimated[20] to be about $10^{(2+0.4\nu)}$ that in our case gives $N_{min} \approx 1000$, which is well below the number of experimental points we have.

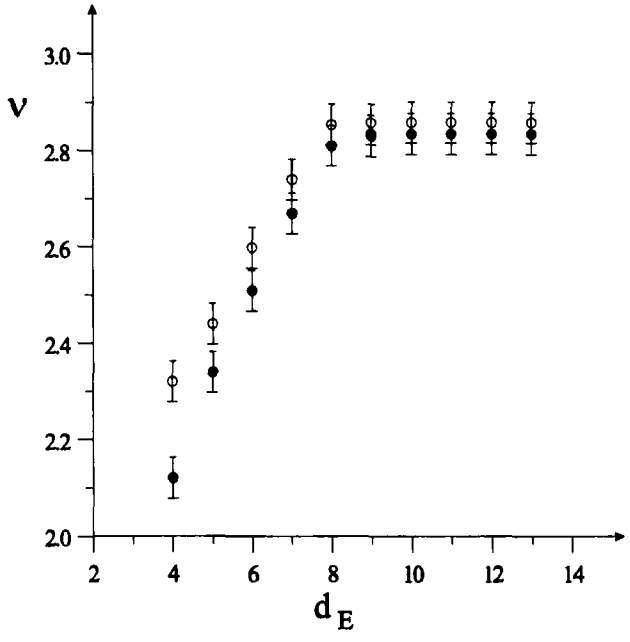

FIGURE 6: Information dimension vs. the embedding dimension both for $I_\perp$ (dark points) and $I_{//}$ (white points).

The second task towards a global characterization of the attractor consists in determining the Lyapunov exponents, which represent a measure of the average exponential rates of

divergence or convergence of nearby orbits in the phase space[13]. This means that the Lyapunov exponents characterize the sensitive dependence of a dynamic system upon the initial conditions, a characteristic shared by almost all the chaotic dynamic systems. Indeed, in a chaotic system, neighboring orbits in the phase space diverge exponentially, so that the chaoticity of the attractor is unambiguously proved if at least the largest Lyapunov exponent λ is greater than zero. It is a simple matter to realize that, if the dynamic system is represented by a set of nonlinear differential equations, the Lyapunov exponents can be easily calculated, whereas to get the spectrum of the exponents from an experiment is more difficult. In the last years some methods to estimate the complete spectrum of the Lyapunov exponents appeared in the literature[21]. However in the present paper we are interested only in the discrimination between the chaotic and the periodic regimes, so that the estimation of the maximum Lyapunov exponent suffices. We have estimated the values both of $\lambda(I_{\perp})$ and $\lambda(I_{//})$ by using an algorithm similar to that developed by Wolf et al.[22]. Starting from an initial point $\vec{x}(I,t_0)$ on the attractor, we have calculated the distance $L(t_0)$ from the nearest neighbor. At a later time t_1 the initial length has evolved to a length $L'(t_1) \approx 2^{\lambda(t_1-t_0)} L(t_0)$. Therefore by using a replacement point and iterating M times this procedure, we obtain an estimate of the maximum Lyapunov exponent as:

$$\lambda \approx \frac{1}{t_M - t_0} \sum_{k=1}^{M} \log_2 \frac{L'(t_k)}{L(t_{k-1})}$$

The temporal convergence of λ, as a function of the evolution time on the attractor, is shown in the figures 7 and 8, for $I_{//}$ and $I_{\perp}$ respectively. The curves refer to the embedding dimension $d_E = 8$, since if d_E goes much beyond the minimally required value, a contamination of the data might happen[22]. We indicate as (a) and (b) the curves that refer to the chaotic regime, which have been calculated by a replacement time of 5 seconds (a) and 1 second (b). The Lyapunov exponent related to the attractor of $I_{\perp}(t)$ converges to $\lambda \approx 0.1 \div 0.15$ bits/s., while the exponent related to $I_{//}(t)$ converges to $\lambda \approx 0.03 \div 0.05$ bits/s.. As a comparison we report, in curves (c), the maximum Lyapunov exponent calculated on the attractor both for $I_{\perp}(t)$ and $I_{//}(t)$ when $P_{inc} \approx 540$ mW. As expected

both curves tend to zero, indicating that, for this power of the impinging laser beam, the system is not chaotic . Thus we can assert that the time evaluation of $I_{\perp}(t)$ and $I_{//}(t)$, in cases a) and b), lie on a chaotic attractor, the dynamics becoming unpredictable on a short time scale.

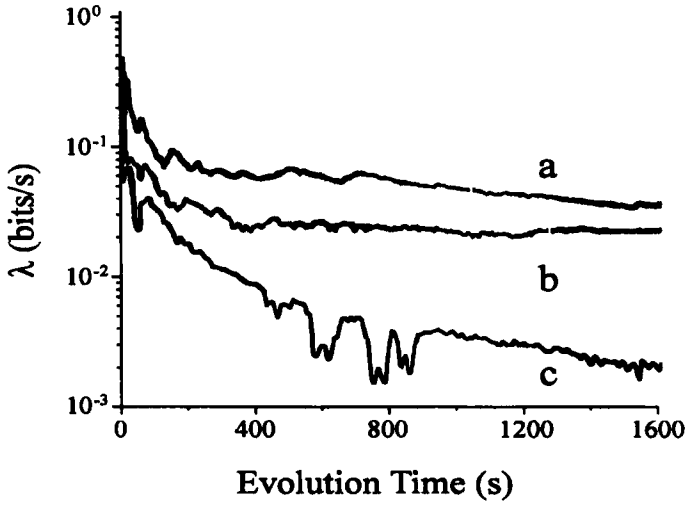

FIGURE 7: Temporal convergence of the maximum Lyapunov exponent λ, as a function of the evolution time on the attractor of $I_{//}$. All curves refer to the embedding dimension $d_E = 8$; curves a) and b) are calculated by a replacement times of 5 s. and 1 s. respectively, and both refer to 700 mW of impinging power (chaotic regime). Curve c) refers to a replacement time of 5 s. and 540 mW of impinging power (quasi-periodic regime).

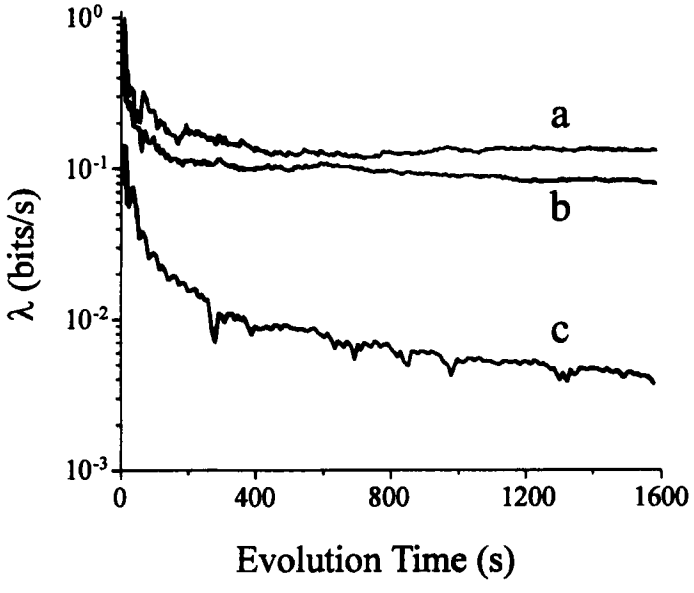

FIGURE 8: Temporal convergence of the maximum Lyapunov exponent λ, vs. the evolution time on the attractor of $I_{\perp}$. All curves refer to the same parameters of figure 7.

EVIDENCE OF TIME INTERMITTENCY IN THE MOLECULAR DIRECTOR DYNAMICS

Let us consider the time series I(t) of duration $T = N\Delta\tau$ measured in the chaotic regime. Even after a large time, the trajectory does not fill the whole phase space. Indeed as the time goes on, the points I(t) belong to a trajectory in the embedding phase space of dimension d_E, which lies on a strange attractor of dimension $d < d_E$. Moreover a kind of stretching and folding process in the ordinary space, that generates the attractor in the

phase space, causes the measure to cover the attractor non uniformly, i.e., the density of the measure I(t) can differ from region to region on the attractor. This can be easily shown by averaging I(t) over a time interval Δt and by repeatedly increasing the interval so that the different length scales of the attractor can be observed.

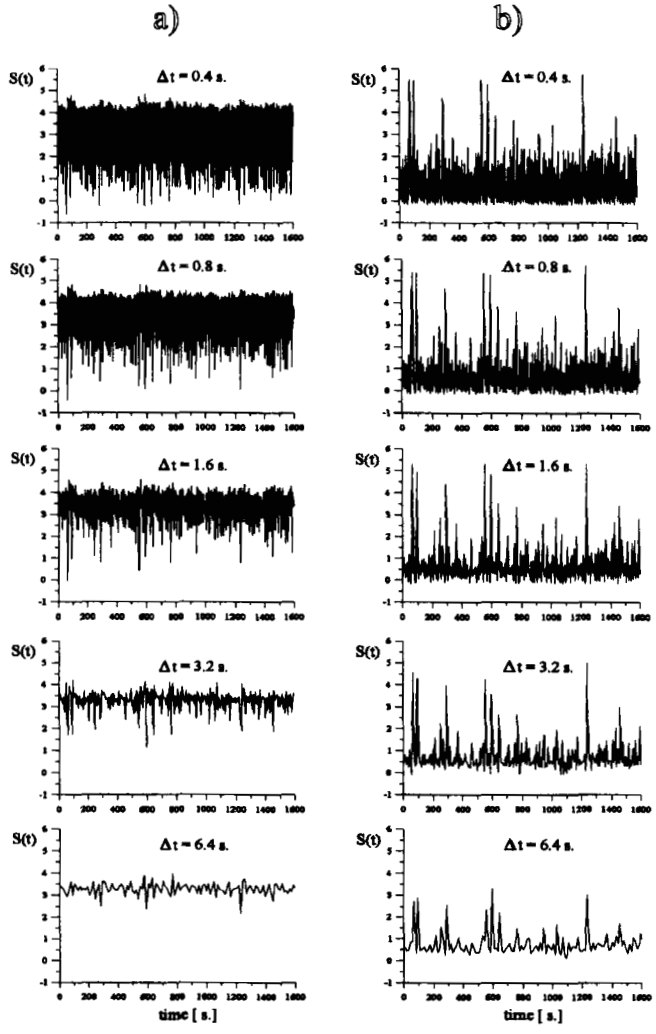

FIGURE 9: Time behavior $S(t) \equiv S[I(t), \Delta t]$ of the signals $I_{//}$ (figure 9a) and $I_{\perp}$ (figure 9b) averaged over different time intervals Δt.

In figures 9a and 9b we show respectively the time evolution of the quantities $S(I_{//}, \Delta t)$ and $S(I_{\perp}, \Delta t)$ defined by

$$S(I, \Delta t) = \frac{1}{\Delta t} \int_{t}^{t+\Delta t} I(s)\, ds \ .$$

It is worthwhile noting some particular features of $S(I_{\perp}, \Delta t)$. First of all the fluctuations of $S(I_{\perp}, \Delta t)$ behave similarly on the different scales. A peak in the curve based on the larger time average tends to be resolved into two or more peaks in the curve corresponding to smaller time averages. This evidence of scale invariance is typical of the fractal structure due to a non uniform covering of the attractor. On the other hand the bursting behavior, which we observe in $S(I_{\perp}, \Delta t)$ on all scales, indicates that the system undergoes to large fluctuations in a small time interval. Indeed the behavior visible in fig. 9b suggests regions characterized by high intensity over small time intervals that are followed by regions of small intensity over large time intervals. These trends indicate that the fluctuations are intermittent in time. We can also observe that the fluctuations are asymmetric with respect to the average intensity, thus reflecting a tail in the intensity distribution and favoring the highest ones. Finally the fluctuations are larger on the smaller scales.

The intermittency of the fluctuations is less evident in $S(I_{//}, \Delta t)$. Indeed in such case (figure 9a) the fluctuations are still asymmetric, but the tail of the intensity distribution is less important, so that the negative fluctuations are favored.

As is well known, the intermittent behavior of a signal is visible when the probability distribution function (PDF) of the signal fluctuations strongly differ from a Gaussian PDF. In figures 10a and 10b we report the PDF's of the intensity fluctuations for $S(I_{//}, \Delta t)$ and $S(I_{\perp}, \Delta t)$ respectively. The PDF's of $S(I_{\perp}, \Delta t)$ show a positive tail both on the largest and the shortest time scales and they seem to be distributed according to a binomial PDF. Conversely, on the shortest time scales, the PDF of $S(I_{//}, \Delta t)$ looks bimodal and almost

Gaussian. Scaling the measure by a largest time interval Δt, the PDF becomes asymmetric and unimodal, exhibiting a tail of negative fluctuations.

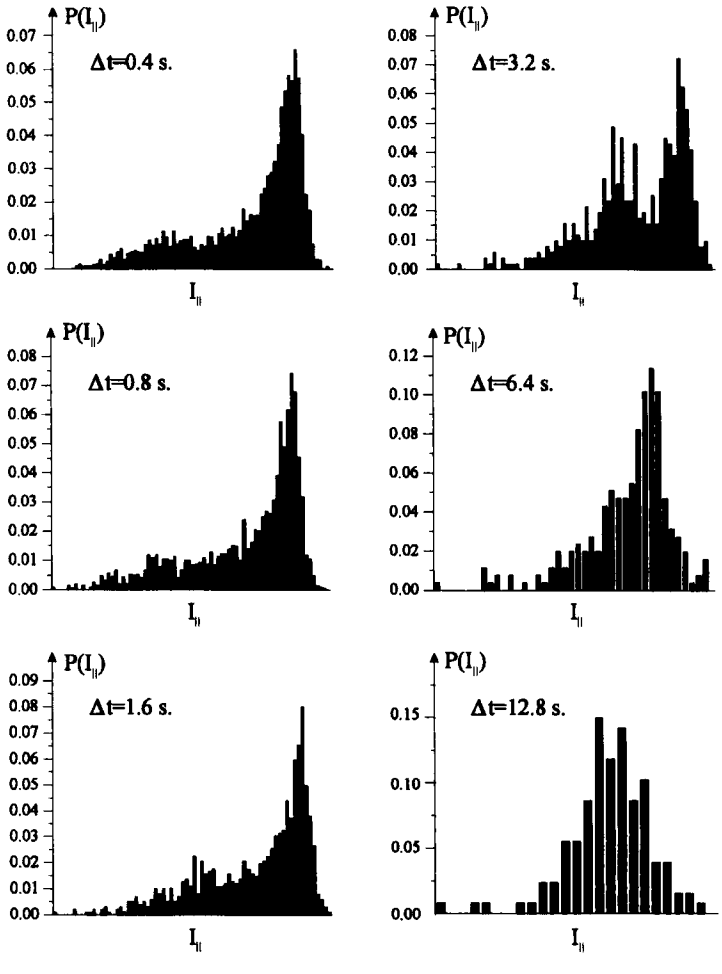

FIGURE 10a: Probability distribution functions P(I) of S(t), for the signals $I_{//}$ for different time intervals Δt.

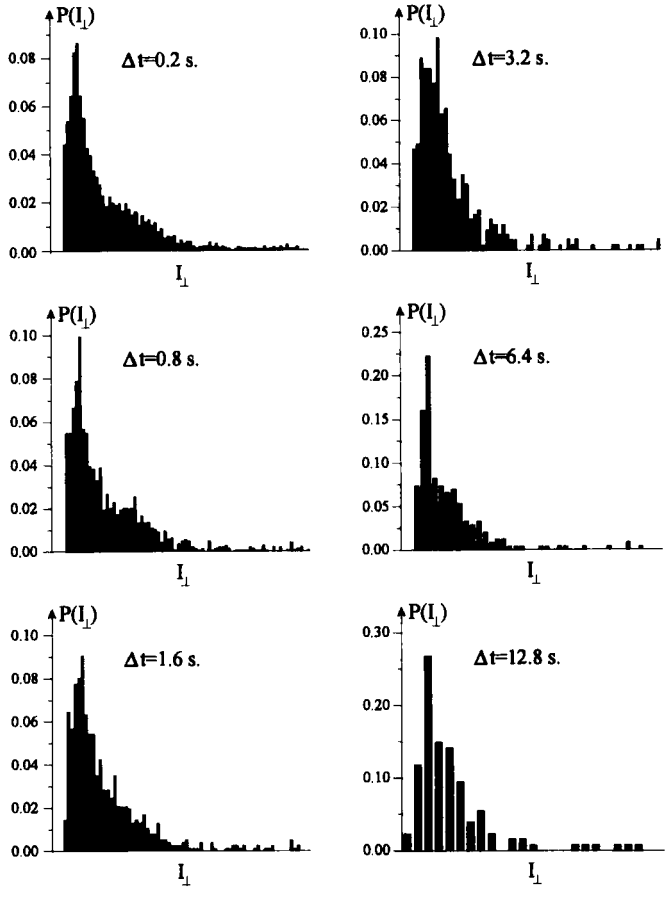

FIGURE 10b: Probability distribution functions P(I) of S(t), for the signals $I_\perp$ for different time intervals Δt.

In figure 11 we quantify our remarks by plotting vs. Δt the kurtosis k(δS) and the skewness Σ(δS) defined by:

$$k(\delta S) = \frac{\langle \delta S^4 \rangle}{\langle \delta S^2 \rangle^2} \quad \text{and} \quad \Sigma(\delta S) = \frac{\langle \delta S^4 \rangle}{\langle \delta S^2 \rangle^{\left(\frac{3}{2}\right)}}$$

where $\delta S = S - \langle S \rangle$, the brackets being the average over the total number of points of $S(I, \Delta t)$, say $T/\Delta t$.

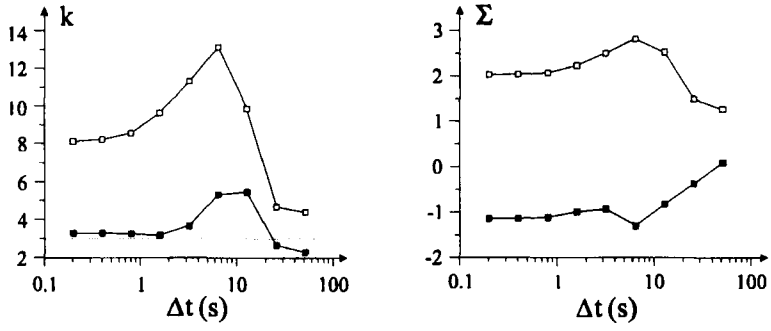

FIGURE 11: Kurtosis k and skewness Σ of S(t) for the signals $I_{//}$ (black points) and $I_{\perp}$ (white points) as functions of Δt. Dotted lines indicate k and Σ for the Gaussian distribution.

On all the time scales the kurtosis of $\delta S(I_{\perp})$ exceeds the value of 3, which is the value expected for a Gaussian distribution, so unambiguously revealing the intermittent nature of the fluctuations of $I_{\perp}(t)$. The kurtosis of $\delta S(I_{//})$ on the other hand, slightly differs from 3 on almost all the time scales, so confirming its Gaussian, even if bimodal, nature. It is worth noting that the kurtosis $k(\delta S)$, calculated for $\delta S = \delta\left[S(I_{\perp}) + S(I_{//})\right]$, is about 3 on all the time scales. Hence we expect $I_{\perp}(t)$ to be relevant for the study of the structure of the attractor. The skewness $\Sigma(\delta S)$ indicates the same deviates from a Gaussian distribution.

Both the PDF's of $S(I_{\perp}, \Delta t)$ and $S(I_{//}, \Delta t)$ are asymmetric, but the skewness of $\delta S(I_{\perp})$ is greater than that of $\delta S(I_{//})$ on all the time scales.

MULTIFRACTAL STRUCTURE OF THE ATTRACTOR

In this section we will deal with the problem of giving a characterization of the structure of the attractor of $I(t)$, with the aim of getting more insight into the physical process that generates the intermittency illustrated above.

Let us consider the q-th power of $S(\Delta t) = S(I, \Delta t)$, say $\langle [S(\Delta t)]^q \rangle$. In the phase space each measure $S(\Delta t)$ lies on a certain region of the attractor, hence positive values of q emphasize small scale fluctuations of the attractor, while negative values of q evidence the large ones. Despite the self similar behavior of figures 10, we assume[14] a set of scaling exponents $\kappa(q)$ for the q-th power of $S(\Delta t)$:

$$\langle [S(\Delta t)]^q \rangle \approx \left(\frac{\Delta t}{T}\right)^{\kappa(q)} \tag{1}$$

The study of the curve $\kappa(q)$ gives information on the fractal structure of the attractor. For a homogeneous fractal of dimension D_F independent of the scales, it can be shown[14] that $\kappa(q) \approx q D_F$. If the fractal is non-homogeneous the dimension D_F depends on q, so that $\kappa(q)$ is a nonlinear function of q. From a theoretical point of view, the existence of either fractal or multifractal structure, can be described by introducing a set of scaling exponents α, which depend on q. We say that, in the limit $(\Delta t / T) \to 0$, the q-th power of the structure function is singular with a singularity α. If the attractor shows a fractal structure, there exists a single singularity with scaling α, while if a multifractal structure is present, we must account for an entire spectrum of singularities for $S(\Delta t)$.

Let us assume that the singularities can be characterized by a continuous range of scaling exponents $\alpha(q)$. For any $\alpha(q)$, a set Θ_α exists, whose dimension is $f(\alpha)$, such that, for $\Delta t \in \Theta_\alpha$, $S(\Delta t)$ behaves as

$$S(\Delta t) \approx \left(\frac{\Delta t}{T}\right)^{\alpha-1}.$$

The set of the dimensions $f(\alpha)$ is called the singularity spectrum[15].

Let us look for the number of boxes, in the phase space, in which the variable $\alpha(q)$ assumes values within the range α' and $\alpha'+d\alpha$. If $\rho(\alpha)$ is the density of the measure, the number of boxes is given by

$$N(\alpha)\,d\alpha \approx \rho(\alpha)\,d\alpha\left(\frac{\Delta t}{T}\right)^{1-f(\alpha)}$$

$(\Delta t / T)^{1-f(\alpha)}$ being the total number of boxes occupied by the fluctuations scaled on Δt. Then the value of the q-th moment of $S(\Delta t)$ can be calculated by integrating all over the values of $\alpha(q)$

$$\left\langle [S(\Delta t)]^q \right\rangle \approx \int N(\alpha)\,d\alpha\left(\frac{\Delta t}{T}\right)^{q[\alpha-1]} \approx \int \rho(\alpha)\,d\alpha\left(\frac{\Delta t}{T}\right)^{[q(\alpha-1)+1-f(\alpha)]}$$

In the limit of small values of $(\Delta t / T)$ the integral can be calculated by using a saddle-point technique, that is the integrand results proportional to a Gaussian centered around the value $\bar{\alpha}$ that minimizes the exponent $[q(\alpha-1)+1-f(\alpha)]$. Then the integral is proportional to $(\Delta t / T)^{[q(\alpha-1)+1-f(\alpha)]}$ evaluated at the minimum value of the exponent.

By comparison with eq. (1) we can write the relation:

$$\kappa(q) = \min_\alpha \{q(\alpha-1)+1-f(\alpha)\}$$

From the right hand side term of the last equation we obtain the value $\bar{\alpha}$ by the relation $\partial f / \partial \alpha = q$ when $\partial^2 f / \partial \alpha^2 < 0$, and we obtain the fundamental equation describing the multifractal structure of the attractor:

$$f(\alpha) = q(\alpha-1)+1-\kappa(q) \tag{2}$$

where

$$\alpha(q) = \frac{d}{dq}\left[(q-1)D_q\right] \tag{3}$$

and

$$D_q = \frac{\kappa(q)}{q-1} + 1 \; ; \tag{4}$$

these are the set of generalized dimensions introduced by Hentschel and Procaccia[23].

In order to apply this analysis to our case, we can extract a direct measure of $\kappa(q)$ from the experimental data; then by eq.s (3) and (4) the value of q univocally select a value of α, so that from eq. (2) we get an experimental measure of the singularity spectrum.

To explicitly calculate the scaling exponents of the structure function, we proceed as follows. For a given time scale Δt, we compute $[S(\Delta t)]^q$, in the range $-10 \le q \le 10$. We repeat the computation of $[S(\Delta t)]^q$ for different values of Δt, and for each of these time series we compute the average $\langle [S(\Delta t)]^q \rangle$. Then, on the basis of eq. (1), from the plot of $\ln\{\langle [S(\Delta t)]^q \rangle\}$ as a function of $\ln(\Delta t / T)$, we fit the exponent $\kappa(q)$ along with its uncertainties by a least square method over the linear range, the exponent $\kappa(q)$ along with its uncertainties. In figure 12 the curves $\kappa(q)$ vs q are reported both for $S(I_\perp, \Delta t)$ and $S(I_{//}, \Delta t)$. We note that, while the curve pertinent to $I_{//}(t)$ is roughly linear, the curve relative to $I_\perp(t)$ is nonlinear, thus indicating that the attractor relative to $I_\perp(t)$ has a multifractal structure. For this reason, in the following we restrict our attention to $I_\perp(t)$. In the range $-4 \le q \le 4$, where the uncertainties are relatively small, the experimental curve $\kappa(q)$ for $I_\perp(t)$ can be approximated by the 5-th degree polynomial

$$\pi(q) \approx -1.8 \times 10^{-3} q^5 + 4.5 \times 10^{-3} q^4 + 4.3 \times 10^{-2} q^3 - 0.27 q^2 + 0.22 q + 2.09 \times 10^{-2}$$

which is also shown in figure 12.

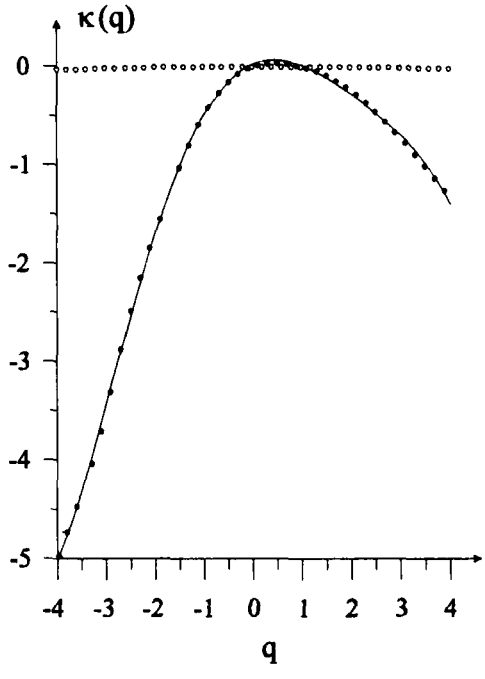

FIGURE 12: Plot of the scaling exponent $\kappa(q)$ vs. the q-th power of S(t). Dark and white dots refer respectively to $I_{\perp}$ and $I_{//}$. The curve $\kappa(q)$ calculated for $I_{//}$ is independent on q, whereas the curve calculated for $I_{\perp}$ has been approximated by the 5-th degree polynomial $\pi(q)$ reported in the text and shown by the full line in the figure.

By using the Legendre transformations (2) and (3), we have calculated the singularity spectrum and obtained the points shown in figure 13. In the same figure we report the curve $f(\alpha)$ obtained from the sine-circle map at the crossing from the quasi periodic to the chaotic regime[15]. Since our data give rise to a broader curve, in agreement with to other

experimental determinations[24] of $f(\alpha)$, we deduce that our signal $I_{\perp}$ crossed the critical line that distinguishes the quasi periodic motion from the chaotic one.

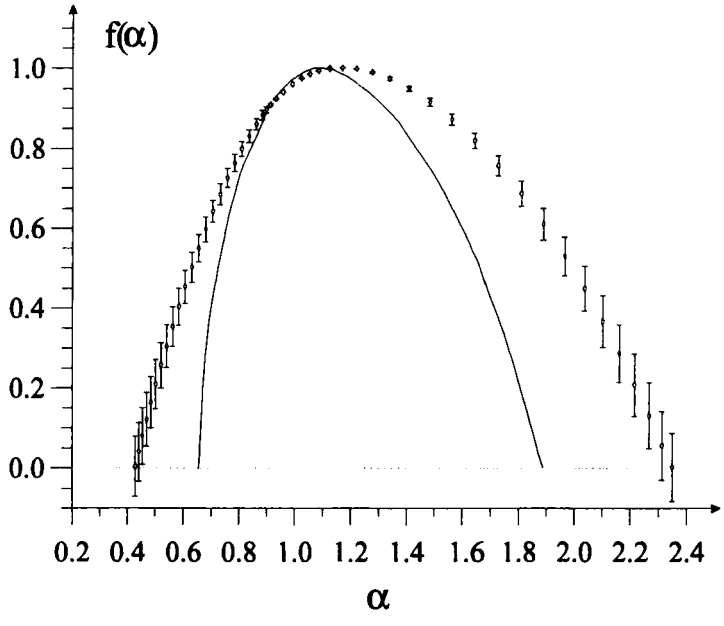

FIGURE 13: Singularity spectrum $f(\alpha)$ calculated for $I_{\perp}$ along with its uncertainties. The full line refers to the singularity spectrum obtained from the sine-circle map at the crossing from the quasi periodic to the chaotic regime.

Let us consider some features of the curve $f(\alpha)$. As is shown in figure 13, the singularity spectrum assumes its maximum $f(\alpha_{max}) \cong 1$ when $\alpha_{max}(q = 0) \cong 1.17$, i.e., the strength of the singularity α that lies in the majority of the box is greater than one. There are two characteristic points of the curve $f(\alpha)$: the point $f(\alpha = 1)$ and the point $f(\alpha) = \alpha$. The former represents the dimension of the set where all the singularities of $S(\Delta t)$ are located,

while the latter point represents the dimension of the set where the moment $S(\Delta t)$ is concentrated asymptotically. From the Legendre transformations (2)-(4) it can be found that the point $f(\alpha) = \alpha$ corresponds to the set whose dimension is D_1. In our case $f(\alpha = 1) \approx 0.97$ and $D_1 = 0.90$, i.e., both sets are almost space filling. Moreover the dynamics shows the region of latent singularities[25] defined by $f(\alpha) < 0$; in our case this region occurs for $\alpha \leq 0.43$ and $\alpha \geq 2.34$. The condition of negative dimension of the set Θ_α simply means that there is typically less than one box in a sample corresponding to these values of α.

Finally, to characterize the intermittency, it is useful to introduce[26] the intermittency exponent μ as the rate of increase of the variance σ^2 of $\mathrm{Ln}(S_\tau)$ as a function of $\mathrm{Ln}(\tau / T)$, i.e., $\sigma^2 = \mu \mathrm{Ln}(\tau / T)$. In other words μ is a measure of the rate of increase of the tails of the PDF's with respect to a Gaussian PDF.

The exponent μ is closely related[27] to the scaling exponents curve $\kappa(q)$ of the multifractal formalism by the relation $\mu = -\left[\frac{d^2}{dq^2} k(q)\right]_{q=0}$. In our case the intermittency exponent is within the range 0.48 ± 0.04.

CONCLUSIONS

In this paper we report the study of the multifractal structure of the attractor that produces in the phase space $\left(I, \frac{dI}{dt}\right)$ during the phenomenon of the molecular director reorientation induced by an intense optical field. When the intensity of the impinging laser beam increases, both the components of the transmitted light with polarization parallel and perpendicular to the incident polarization show a transition towards a chaotic regime through several dynamic states, whose behavior is not yet completely clarified[12]. For the chaotic regime, we summarize the main results we have obtained:

1) We have calculated, both for $I_{\perp}$ and $I_{//}$, the fractal dimension of the attractor and estimated the maximum Lyapunov exponent, showing that the motion in the phase space becomes chaotic for $P_{inc} > 700$ mW. The characteristic times over which the dynamics becomes unpredictable are of the order of 10s. for $I_{\perp}$, and 33s. for $I_{//}$.

2) In the chaotic regime, the flow in the phase space does not uniformly fill the attractor, thus showing that the observed phenomenon is intermittent. This implies that, when the directors dynamics is viewed over different time scales, some regions of the phase space are more filled than others. Since this reflects, even if in a complicated way, the real motion of the molecular director in the space, we can conclude that the intermittency indicates the presence of regions of the space where the director "prefers" to reside. The intermittency is evident if we analyze the PDF's and the kurtosis of the fluctuations δI. The PDF's look very different from Gaussian PDF's, and the relative kurtosis systematically exceed the value of three. We remark that the intermittency is much more evident in $I_{\perp}(t)$ than in $I_{//}(t)$. The reasons of this asymmetry might be related to the nonlinear coupling between $I_{\perp}(t)$ and $I_{//}(t)$ which can be different in different experimental geometries.

3) In order to look for a multifractal structure of the attractor we have fitted the time-average of the q-th power of $S(\Delta t)$, say $\langle [S(\Delta t)]^q \rangle$, at different scales $\Delta t / T$, by a power law with exponent $\kappa(q)$. We found a nonlinear $\kappa(q)$ only for $I_{\perp}$, so that only in this case it is possible to find a multifractal structure. Indeed we have introduced a continuous set of scaling exponents $\alpha(q)$ for $\langle [S(\Delta t)]^q \rangle$ and, using the measured values of $\kappa(q)$, we have calculated the set of generalized dimensions D_q and the singularity spectrum $f(\alpha)$. These curves have the characteristic shape of those found in other multifractal structures[14,15,24].

The results we have found show the experimental evidence of intermittency in the phenomenon of molecular director reorientation and our analysis is useful to gain more insight into this phenomenon. On the other hand our calculations could open a new way to a theoretical understanding of the reorientation in terms of a better modelling of the interaction between the radiation and the matter.

Let us consider, for example, a simple conceptual model, which is intended only to illustrate qualitatively how the interaction between the radiation and the matter might produce multifractal fluctuations of $I_{\perp}(t)$. Indeed it is well known that the motion of the molecular director can be interpreted in terms of the exchange of angular momentum and energy between the radiation and the matter. As in the case of intermittent fluid flows, in which, due to the nonlinear interactions, the energy flux through the various scales is not uniform[27,28], we can assume that the same kind of asymmetric exchange happens between the radiation and the matter for a certain measure $\Psi(I)$. If in fact this is the case, a binomial multiplicative model for $\Psi(I)$ can be built up, which is based on a two-scale Cantor set with equal partition intervals. From such a model it can be found[27,28] that

$$D_q = \frac{\log_2\left[\xi^q + (1-\xi)^q\right]}{1-q} \tag{5}$$

where $0 < \xi < 1$ is an external parameter that measures the non-uniformity of the exchange of $\Psi(I)$, i.e. the intermittence strength. When $\xi = 0.5$ the process is not intermittent, while on the contrary if ξ assumes extreme values, the process is strongly intermittent. We have fitted the measured values of $\kappa(q)$ by eq. (4) with D_q given by eq. (5), and we show in figure 14 the curve $\kappa(q)$ along with the theoretical curve corresponding to the best fit, obtained for $\xi = 0.193 \pm 0.002$. The model provides, despite our ignorance of the measure $\Psi(I)$, a good agreement for $-10 \le q \le 2$, while as concerning high q values the theoretical curve is slightly below the experimental one. This can be ascribed to the fact that, on emphasizing the smallest scales, i.e., looking at the highest q, we observe fluctuations that are more intense than those our simple model can account for. The same trend can be observed in figure 15, in which we report the experimental and theoretical curves of D_q. It is worth noting that the experimental points lie inside the theoretical extreme values $D_{-\infty} = \log_2 \xi^{-1} = 2.37$ and $D_{+\infty} = \log_2 (1-\xi)^{-1} = 0.31$, as shown in the figure. Hence, a simple fragmentation model can give rise to results that agree with our experiments.

Obviously this simple model does not address the very rich dynamic process that is involved in the experimental situation. However we think this could be a way to a better understanding of the phenomenon.

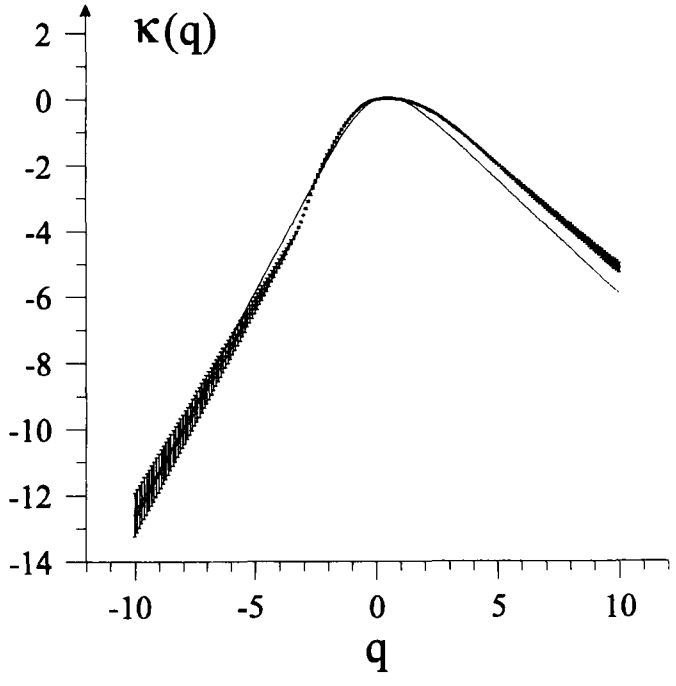

FIGURE 14: Plot of the scaling exponent $\kappa(q)$ vs. the q-th power of S(t) calculated for $I_{\perp}$. Also shown is the theoretical curve (full line) obtained by eq. 5, which corresponds to the best fit of the intermittency parameter $\xi = 0.193 \pm 0.002$.

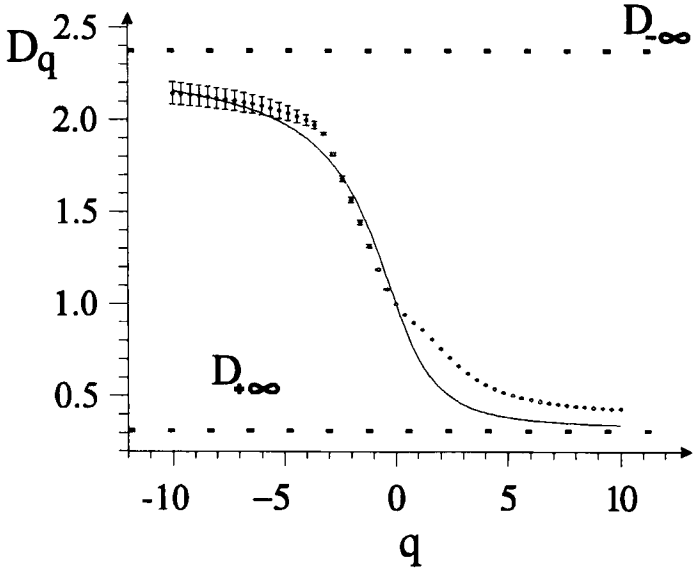

FIGURE 15: Plot of the generalized dimension D_q (white points) calculated for $I_\perp$, along with the theoretical curve (full line) obtained by eq. (5) for $\xi = 0.193 \pm 0.002$. It is also show the asymptotic theoretical points $D_{-\infty}$ and $D_{+\infty}$ (dotted line) obtained for the above mentioned values of ξ.

REFERENCES

1. G.Vertogen and W.H de Jeu, Thermotropic Liquid Crystals, Fundamentals, edited by F.P.Schäfer, (Springer-Verlag Berlin 1988).
2. L.M.Blinov, Electro-optical and magneto-optical properties of liquid crystals, (J.Wiley & sons New York 1981).
3. N.A.Tabiryan, A.V.Sukhov and B.Ya Zel'dovich, The Orientational Optical Nonlinerity of Liquid Crystals in Mol. Cryst. Liq. Cryst. special topics XIX (1986)

4. F.Bloisi, R.Vicari, F.Simoni, G.Cipparrone, C.Umeton, Jour. Opt. Soc. Am. 5, 2462 (1988)
5. A.S.Zolot'ko and V.F.Kitaeva, Sov. Phys. JETP 64, 76 (1986)
6. E.Santamato, M.Romagnoli, M.Settembre, B.Daino and Y.R.Shen, Phys. Rev. Lett. 61, 113 (1988)
7. E.Santamato, G.Abbate, P.Maddalena, L. Marrucci and Y.R.Shen, Phys. Rev. Lett. 64, 1377 (1990)
8. L.Marrucci, G.Abbate, S.Ferraiuolo and P.Maddalena, Phys. Rev. A 46, 4859 (1992)
9. A.S.Zolot'ko, V.F.Kitaeva, N.Kroo, N.N.Sobolev and L.Czillag, Sov. Phys. JETP Lett. 32, 158 (1980)
10. A.S.Zolot'ko, V.F.Kitaeva, N.Kroo, N.N.Sobolev, A.P.Sukhorukov, V.A. Troshkin and L.Czillag, Sov. Phys. JETP 60, 488 (1984)
11. V.F.Kitaeva, N.Kroo, N.N.Sobolev, A.P.Sukhorukov, V.Yu Federovich and L.Czillag, Sov. Phys. JETP 62, 520 (1985)
12. G.Cipparrone, V.Carbone, C.Versace, C.Umeton, R.Bartolino and F.Simoni, Phys. Rev. E 45, 3741 (1993)
    V.Carbone, G.Cipparrone, C.Versace, R.Bartolino, C.Umeton and N.V.Tabiryan, Mol. Cryst. Liq. Cryst. 251, 167 (1994)
    V.Carbone, G.Cipparrone, C.Versace, C.Umeton and R.Bartolino, Multifractal Structure and Intermittency of Laser-Generated Turbolence in Nematic Liquid Crystals, Phys Rev E in press
13. J.P.Eckmann and D.Ruelle, Rev. Mod. Phys. 57, 617 (1985)
14. G.Paladin and A.Vulpiani, Phys. Rep. 156, 147 (1987)
15. T.C.Halsey, J.M.H.Kadanoff, L.P.Procaccia and B.I.Shroiman, Phys Rev. A, 33, 1141 (1986)
16. F.Takens, Lecture Notes in mathematics 898, 230 (1981)
17. D.Ruelle, Proc. Royal Soc. London Ser. A427, 241 (1990)
18. N.H.Packard, J.P.Crutchfield, J.D.Farmer and R.S.Shaw, Phys. Rev. Lett. 45, 712 (1980)
19. P.Grassberger and I.Procaccia, Phys. Rev. Lett. 50, 346 (1983)
20. H.A.Neremberg and C.Essex, Phys. Rev. *A* 42, 7065 (1990)
21. J.P.Eckmann, S.O.Kamphorst, D.Ruelle and S.Ciliberto, Phys. Rev. A 34, 4971 (1986)
    M.Sano and Y.Sawada, Phys. Rev. Lett. 55, 1082 (1985)
    R.Brown, P.Bryant and H.D.I. Abarbenal, Phys. Rev. A 43, 2787 (1991)
22. A.Wolf, J.B.Swift, H.L.Swinney and J.A.Vastano, Physica 16D, 285 (1985)
23. H.G.E.Hentschel and I.Procaccia, Physica 8D, 435 (1983)
24. Z.Su, R.W.Rollins and E.R.Hunt, Phys. Rev. E, 40, 2689 (1989)
25. B.B.Maldelbrot, Pure Appl. Geophys. 131, 5 (1989)
26. A.N.Kolmogorov, J. Fluid Mech. 13, 82 (1962)
27. C.Meneveau and K.R.Sreenivasan, J. Fluid Mech. 224, 429 (1991)
28. V.Carbone, Phys Rev. Lett. 71, 1546 (1993)